Manufacturing of a freeform phase plate for suppression of diffraction in an astronomical telescope

Gregg E. Davis*[a], Matthew A. Kenworthy[b], Alan R. Hedges[a]
[a]II-VI Incorporated, 375 Saxonburg Boulevard, Saxonburg, PA, USA, 16056
[b]Steward Observatory, 933 North Cherry Avenue, Tucson, AZ, USA, 85721

ABSTRACT

The addition of a high resolution encoder to the spindle of a standard diamond turning lathe has allowed for precision control of angular rotation. With three precision controlled axes, (rotational C, linear X and linear Z), tool path programs can be defined in cylindrical coordinates, which enables the production of freeform geometries. Optical designers are now exploring complex shapes that were previously unachievable. These shapes range from long radius toroids to freeform wavefront corrector plates. From a manufacturing point of view, interfacing between optical design programs, fabrication equipment, and metrology equipment often proves to be the most difficult part of the production process. The optical design must be translated into a tool path for the diamond turning lathe, and in some cases the design must be imported into the metrology software for surface comparison. The purpose of this report is to inform the reader about some of these manufacturing challenges using one specific example: a freeform phase plate that suppresses diffraction in an astronomical image and enhances searches for extrasolar planets around nearby stars. Designed by Johnan Codona and Roger Angel from the University of Arizona, this ZnSe lens has many ridges and valleys that have been optimized to reduce the 4 micron wavelength light observed from a nearby star to a level that makes planet detection possible. The phase plate had an aperture of 4.44mm and was placed on a 12.7mm diameter 4mm thick substrate. Surface feature size was approximately 2.5 micron peak-to-valley. In on-sky testing, the optic attenuated diffracted light from the star approximately 100 fold.

Keywords: diamond turning freeform metrology infrared extrasolar planet diffraction suppression telescope

1. INTRODUCTION

In the year 2006, II-VI Inc. produced several freeform phase plates for the Steward Observatory. These optics (designed by Johnan Codona and Roger Angel) suppress diffraction in an astronomical image and aid the search for extrasolar planets around nearby stars. This paper describes the technical challenges involved with the production of these phase plates.

The science behind diffraction suppression and how the designers arrived at the freeform surface is beyond the scope of this paper. Pertinent to this report, however, are the final design requirements which can be summarized as follows:

1. Optic must transmit 4 micron wavelength light
2. Side 1 has an annular aperture (4.44mm O.D. and 1.11mm I.D.) consisting of a freeform surface
3. All light must be blocked outside of the annular aperture
4. Side 2 is plano

The main manufacturing challenge was to transfer the designed freeform surface to the substrate and quantify the deviation from the ideal surface.

2. MANUFACTURING AND MEASUREMENT PROCESS

2.1. General Manufacturing Approach

We started by selecting ZnSe as the optical material. This material is transmissive at the 4 micron design wavelength and it is one that II-VI produces and diamond turns regularly. Since the overall diameter and center thickness were not critical to the design, we selected a standard 12.7mm diameter, 4mm thick, plano/plano window as our starting substrate. To create the annular aperture, a 0.100mm "pedestal" was diamond turned into Side 1 of the optic. No problems were

Optifab 2007: Technical Digest, edited by James J. Kumler, Matthias Pfaff,
Proc. of SPIE Vol. 10316, 1031613 · © 2017 SPIE
Optifab 2007: Technical Digest, SPIE Technical Digest TD04
(2007) 0277-786X/07/$18 doi: 10.1117/12.718731
CCC code: 0277-786X/17/$18 · doi: 10.1117/12.718731

encountered during the machining of the outer diameter of the pedastal, however, the inner diameter required a special tool setup to minimize undercutting. After the pedestal was diamond turned, Side 1 of the part was coated with gold. The freeform surface was then diamond turned into the pedestal, leaving the gold coating everywhere else on Side 1. A registration fiducial was also placed at the edge of the Side 1 by dragging the diamond tool with the spindle locked. The final step was to place an anti-reflection coating on both sides of the optic. The general manufacturing approach is illustrated in figure 2.1.

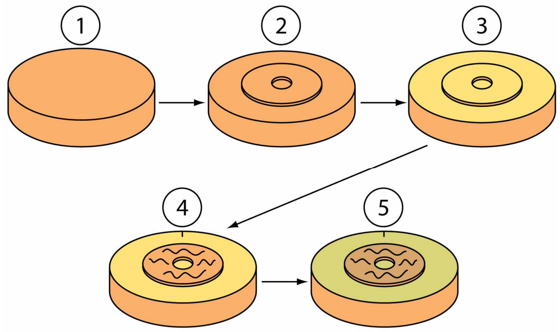

Figure 2.1: Illustration of the general manufacturing approach. 1) Start with plano/plano ZnSe substrate. 2) Diamond turn pedestal into Side 1. 3) Gold coat Side 1. 4) Diamond turn freeform surface onto pedestal and make fiducial mark. 5) Coat both sides with anti-reflective coating.

2.2. Freeform Surface Generation

The main manufacturing challenge was to transfer the designed freeform surface to the substrate and quantify the deviation from the ideal surface. In this case, the optical design was received as set of x,y,z point data covering a 5.6mm x 5.6mm square area with 0.0222mm point spacing. The surface was rippled and had a peak-to-valley of about 2.5 microns (after scaling for the index of refraction for ZnSe at $\lambda = 4$ micron). Typically an x-y polynomial or set of Zernikes would adequately approximate a freeform surface, but in this case the order of the approximation would have been exceedingly high. Instead we opted for an interpolative approach.

The interpolation algorithm that we used is relatively straightforward, and the setup is illustrated in Figure 2.2. The algorithm uses the current x,y position to determine which square on the grid of points encloses that position. The z-positions of the four points on the square are individually weighted and summed to determine the overall z-position. The weighting factors of the four points are based on their relative distances from the current x,y location, and it is also important to note that the sum of the four weighting factors always equals one. The equations of the four weighting factors are listed in Eq 2.1a-d

$$w_{00} = \left(\frac{x_{inc} - x_{local}}{x_{inc}} \right) \cdot \left(\frac{y_{inc} - y_{local}}{y_{inc}} \right) \tag{2.1a}$$

$$w_{10} = \left(\frac{x_{local}}{x_{inc}} \right) \cdot \left(\frac{y_{inc} - y_{local}}{y_{inc}} \right) \tag{2.1b}$$

$$w_{01} = \left(\frac{x_{inc} - x_{local}}{x_{inc}} \right) \cdot \left(\frac{y_{local}}{y_{inc}} \right) \tag{2.1c}$$

$$w_{11} = \left(\frac{x_{local}}{x_{inc}} \right) \cdot \left(\frac{y_{local}}{y_{inc}} \right) \tag{2.1d}$$

The current z-position is calculated by summing the four z-positions of the square after they have been multiplied by their respective weight factors. This calculation is shown in Eq 2.2.

$$z = (w_{00} \cdot z_{00}) + (w_{10} \cdot z_{10}) + (w_{01} \cdot z_{01}) + (w_{11} \cdot z_{11}) \tag{2.2}$$

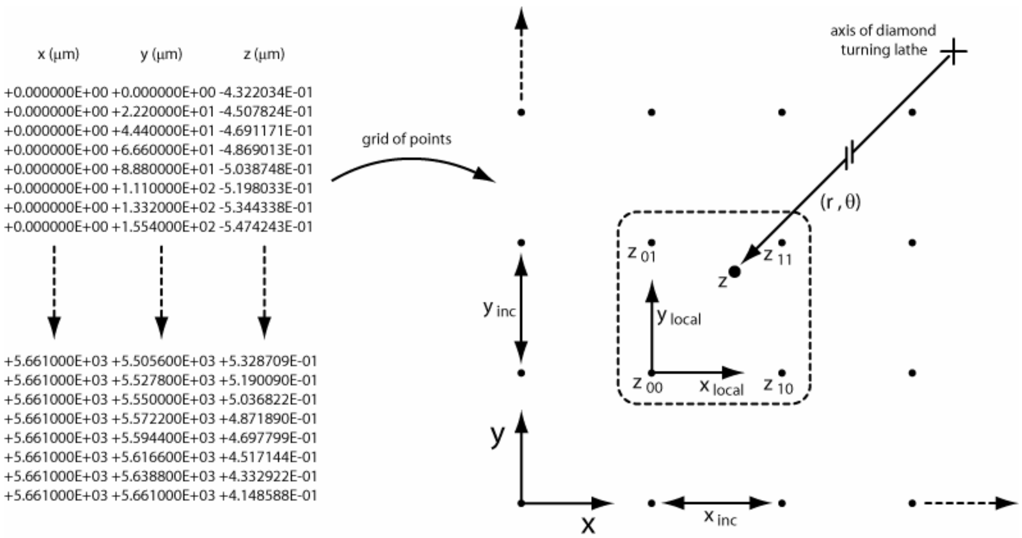

```
    x (µm)          y (µm)          z (µm)

+0.000000E+00 +0.000000E+00 -4.322034E-01
+0.000000E+00 +2.220000E+01 -4.507824E-01
+0.000000E+00 +4.440000E+01 -4.691171E-01
+0.000000E+00 +6.660000E+01 -4.869013E-01
+0.000000E+00 +8.880000E+01 -5.038748E-01
+0.000000E+00 +1.110000E+02 -5.198033E-01
+0.000000E+00 +1.332000E+02 -5.344338E-01
+0.000000E+00 +1.554000E+02 -5.474243E-01

+5.661000E+03 +5.505600E+03 +5.328709E-01
+5.661000E+03 +5.527800E+03 +5.190090E-01
+5.661000E+03 +5.550000E+03 +5.036822E-01
+5.661000E+03 +5.572200E+03 +4.871890E-01
+5.661000E+03 +5.594400E+03 +4.697799E-01
+5.661000E+03 +5.616600E+03 +4.517144E-01
+5.661000E+03 +5.638800E+03 +4.332922E-01
+5.661000E+03 +5.661000E+03 +4.148588E-01
```

Figure 2.2: Illustration of the interpolation setup. The algorithm uses a weighted summation of the four points that enclose the current point to determine the current z-position. The interpolation creates a surface that intersects all of the data and is continuous with position (but not slope).

The weight factors are designed such that if the current location coincides with one of the corners, the weight factors will be (1, 0, 0, 0). Also, if the current location lies on the edge of the square half way between two corners, the weight factors will be (0.5, 0.5, 0, 0). If the current location lies directly in the middle of the square, the weight factors will be (0.25, 0.25, 0.25, 0.25). The weight factors guarantee a surface that intersects all of the ideal point data while having continuous position. The slope is not continuous at the edges of the square, but the small point spacing made this issue negligible.

The algorithm was easiest to implement using Slow Tool Servo (STS) technology since the entire spiral toolpath could be programmed ahead of time without concern for computational efficiency. The STS technology used on this optic manifested itself as a Precitech Nanoform 700 diamond turning lathe with a high resolution encoder on the spindle and some additional software allowing optical surfaces to be defined in cylindrical coordinates. Cutting parameters were set to 32 rpm and 0.5 micron/rev resulting in a 2 hour finish pass. The tool had a 127 micron radius, and a -25º rake angle. Tool radius compensation was applied to the toolpath.

2.3. Surface Measurement

A map of the surface was acquired using a Zygo NewView 5000 white light interferometer. The part was oriented in the field of view using the fiducial as a guide. The measured surface map shown in Figure 2.3 looked very similar to our expectations, but it needed to be quantified. The answer was to import the ideal data into the Zygo Metropro software and subtract the measured surface map from the ideal surface map.

Importation of the ideal data into the Zygo Metropro environment required the creation of a file that the software could access. The first step was to export the measured surface map to an "xyz" file. Using this file as a guide, an ideal xyz file was created over the same x,y locations of the measured file. The interpolation algorithm that was used to program the STS machine was also used to program these ideal measurement points. The ideal xyz file was then converted to a standard Metropro "dat" file, completing the steps necessary to import the ideal surface map. Angular registration of the measured surface to the ideal surface was achieved through the visual alignment of the fiducial, while lateral registration was achieved by forcing the ideal file to be centered in the measured aperture. The ideal surface map was subtracted from the measured surface map within Metropro resulting in the desired error map. The error map revealed a radius error of approximately 2.7 meters in the part, which we speculate to be caused by spindle growth. Since a focal error was not critical to this optic, only one attempt to compensate for radius was made with limited success.

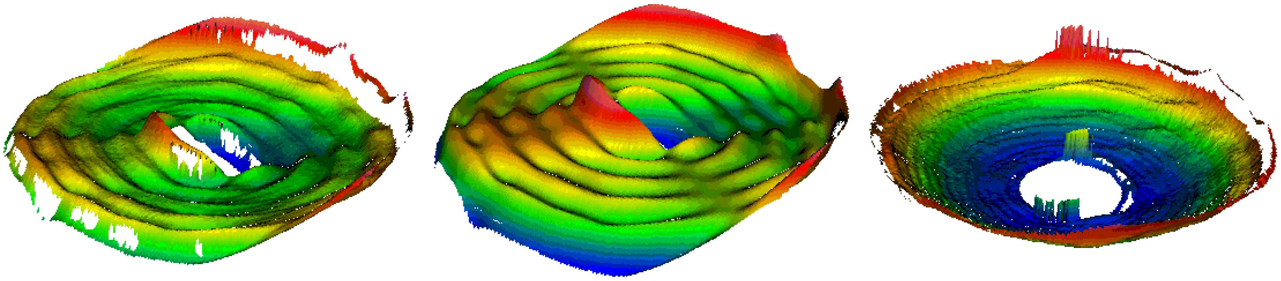

Figure 2.3: Illustration of surface maps: (from left to right) actual surface map, ideal surface map, and error map. The maps are 4.44mm in diameter, and the ideal surface has a peak-to-valley of approximately 2.5 microns. The difference between the actual and ideal maps resulted in an error map with an average radial peak-to-valley error of 815nm (approximated by a 2.7 meter concave best-fit radius of curvature).

3. Final Product

Based on the surface data we have collected and the on-sky test results shown in Figure 3.1, it appears as though we succeeded in manufacturing this freeform phase plate. The on-sky image of a star using this optic compared very favorably with the modeled image of the same star. The actual level of diffraction suppression was approximately 100 fold with this optic, thereby making the detection of extrasolar planets more feasible.

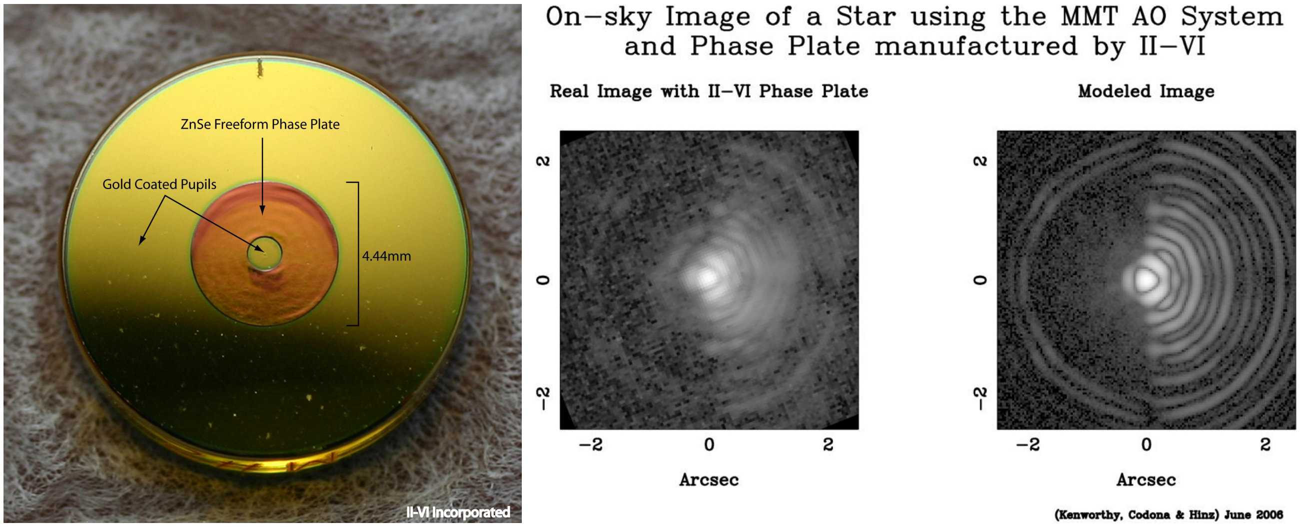

Figure 3.1: Photograph of the freeform phase plate (at left) and the comparison of an on-sky image of a star using this optic with a model using the ideal version of the optic (at right).